IRMPD spectroscopy and quantum-chemical simulations of the reaction products of cisplatin with the dipeptide CysGly

Davide Corinti, Roberto Paciotti, Cecilia Coletti, Nazzareno Re, Barbara Chiavarino, Gilles Frison, Maria Elisa Crestoni, Simonetta Fornarini

IRMPD spectroscopy and quantum-chemical simulations of the reaction products of cisplatin with the dipeptide CysGly

Davide Corinti[a,+]*, Roberto Paciotti[b,+,]**, Cecilia Coletti[b], Nazzareno Re[b], Barbara Chiavarino[a], Gilles Frison[c], Maria Elisa Crestoni[a], Simonetta Fornarini[a]

[a] Dipartimento di Chimica e Tecnologie del Farmaco, Università di Roma "La Sapienza", I-00185 Roma, Italy

[b] Dipartimento di Farmacia, Università G. D'Annunzio Chieti-Pescara, Via dei Vestini 31, Chieti I-66100, Italy

[c]Sorbonne Université, CNRS, Laboratoire de Chimie Théorique, LCT, F-75005 Paris, France

*davide.corinti@uniroma1.it; **r.paciotti@unich.it

[+]The authors contributed equally.

Abstract

The inorganic antineoplastic drug cisplatin was made to react in solution with the dipeptide cysteinylglycine (CysGly), chosen as a functional model of glutathione, and the reaction products were analyzed using electrospray ionization mass spectrometry (ESI-MS). Selected complexes, i.e., the primary substitution product *cis*-$[PtCl(NH_3)_2(CysGly)]^+$ and the chelate *cis*-$[PtCl(NH_3)(CysGly)]^+$, were submitted to IR multiple photon dissociation (IRMPD) spectroscopy obtaining their vibrational features. The experimental IR ion spectra were compared with the calculated IR absorptions of different plausible isomeric families, finding CysGly to bind preferentially platinum(II) via its deprotonated thiolic group in the monovalent complex, *cis*-$[PtCl(NH_3)_2(CysGly)]^+$, and to evolve in the S,N-bound chelate structure *cis*-$[PtCl(NH_3)(CysGly)]^+$ through the SH and NH_2 functionality of the cysteine

residue. Moreover, our findings indicate that the platination reaction does not affect the CysGly peptide bond, which remains in its trans configuration.

These results provide additional insights into the reactivity of Pt(II)-complexes with glutathione which is involved in cellular cisplatin resistance.

Keywords

Antineoplastic drug; platinum complex; structural characterization; IR laser spectroscopy; mass spectrometry; DFT calculations

1. Introduction

Cisplatin, *cis*-$PtCl_2(NH_3)_2$, is among the few inorganic antineoplastic drug still used in therapy and has been a first-choice drug for the treatment of several solid tumors for more than 40 years. Its mechanism of action consists of the formation of intra-strand crosslinks in the DNA by platination of N7 atom of adjacent guanine. Transcription and replication of DNA is thus inhibited eventually leading to cell death.[1-6] The treatment with cisplatin is not free from contraindications. Side effects, in particular gastrointestinal issues,[7-9] and the occurrence of resistance phenomena [10] may limit its use. Second and third generation platinum-based drugs, including carboplatin and oxaliplatin, have partially overcome these problems, but they show at the same time lower success rate and limited applications.[11] Resistance to the drug in the cancer cells is connected to an increase of the production of exporting proteins, a lower expression of membrane copper and organic cation transporters, which are believed to have a fundamental role in the accumulation of cisplatin in the cells, and to an increase in the expression of detoxifying proteins and small peptides.[12,13] Among them, glutathione (GSH) is considered the major contributor to the sequestration of cisplatin. Indeed, as shown in Figure 1, it can directly bind to

the drug both hindering the formation of toxic DNA adducts and increasing the cisplatin efflux from the cells by the GS-X pump as $Pt(GS)_2$ complex.[14-17]

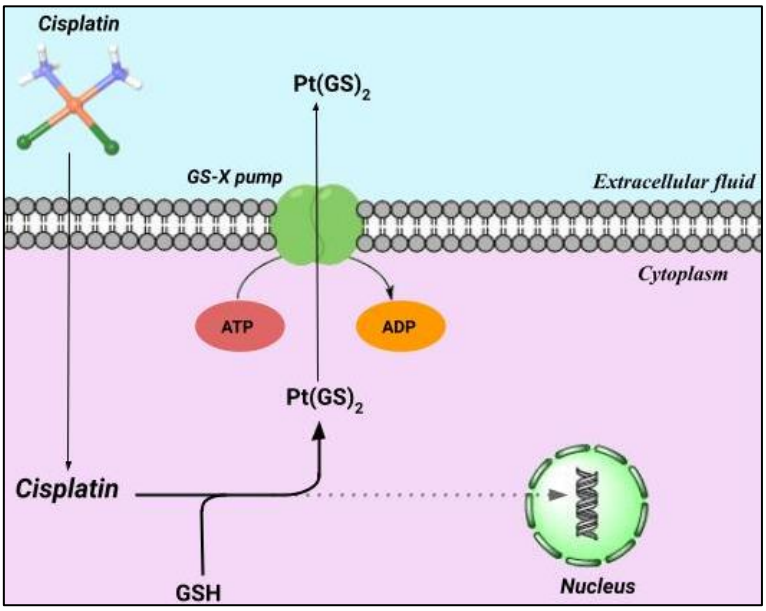

Figure 1. Possible roles of GSH in cisplatin resistance. It can interact with cisplatin promoting the drug elimination mediated by GS-X pump and hindering the formation of therapeutically targeted DNA adducts.

Interaction with amino acid residues in proteins is also an important factor for the distribution of cisplatin in the body and is considered to be related to the appearance of side effects.[18] In agreement with the soft-acid character of Pt(II), amino acid residues presenting sulfur-containing nucleophiles, such as methionine and cysteine, are among cisplatin preferred binding sites together with the nitrogen atom of the histidine imidazole group.[18-26] In spite of being an overlooked topic when compared to the study of cisplatin interaction with nucleotides, it is clear that obtaining more information on the platination of proteins may help to design better Pt-based drugs to overcome some of their limitations.[18] When studied in solution, cisplatin reacts with the amino acids forming a variety of species, with a prevalence of bidentate and dinuclear complexes.[16,28-30] However, thanks to the combined

use of electrospray ionization mass spectrometry (ESI-MS) and IR multiple photon dissociation (IRMPD) spectroscopy, backed by quantum-mechanics calculations, it was possible to identify and characterize the first ionic products of the cisplatin reaction with selected amino acids (AA): *cis*-$[PtCl(NH_3)_2(AA)]^+$, where AA is histidine, methionine or cysteine.[31-33] In particular, ESI-MS has the unique ability to mass-select gaseous ionic intermediates, while its coupling with IRMPD spectroscopy ensures the recording of the vibrational features of ions without any interference from the matrix. Given that ions absorb light only when their vibrational modes are resonant with the impinging photons, by plotting the photodissociation yield as a function of the photon energy an action IR spectrum is produced.[34-38] Comparison with calculated IR spectra of candidate isomers enables the characterization of binding motifs and relevant structural features. This combined approach was found to be well suited to assay biologically relevant metal complexes.[34,35] Indeed, the reaction intermediates of cisplatin with several biological ligands, including amino acids,[31-33,39] but also nucleosides,[40,41] nucleotides[42,43] and small molecules mimicking nucleophilic binding sites in biomolecules,[44,45] were unveiled and fully characterized. In addition, IRMPD spectroscopy was employed to structurally describe cisplatin derivatives in which the ammonia ligands were substituted by amino acids.[46-48] Increasing the molecular complexity of the assayed cisplatin adducts, we have undertaken a multimethodological study of cisplatin complexes with the dipeptide cysteinylglycine (CysGly) in the present paper. It represents the active part of glutathione which also owns an additional glutamic acid residue thus forming a peptide bond with the N-terminus by its γ-carboxylic acid. In addition, exploring the structural features of cisplatin with a dipeptide gives the unique possibility to determine how platination may affect the peptide bond

isomerism.[49,50] IR ion spectroscopy was also exploited to assign the structure of the CysGly radical cation found to be a sulfur radical species,[51] and to study glutathione derivatives.[52-54] In the present paper we report the vibrational and structural characterization of the primary complex of cisplatin with CysGly, *cis*-$[PtCl(NH_3)_2(CysGly)]^+$, and the chelate cis-$[PtCl(NH_3)(CysGly)]^+$, using ESI-MS, IRMPD spectroscopy and DFT calculations. Findings from this study have provided unambiguous evidence for the primary binding site of Pt(II) to CysGly, which can be reliably extrapolated to cysteine-exposing proteins and GSH.

2. Materials and methods

2.1 Materials

Cisplatin and the dipeptide CysGly were research grade products bought from commercial sources (Merck s.r.l. Milan, Italy) and were used without preliminary purification. To produce the complexes of interest, stock aqueous solutions of both CysGly and cisplatin were prepared at 10^{-3} M concentration, subsequently mixed in 1:1 molar ratio and finally diluted in methanol/water (1:1 v/v) to reach a final concentration of $5 \cdot 10^{-5}$ M in each analyte. The cisplatin solution was allowed to stand 24h prior to use to favour aquation of the complex.

2.2 MS and IRMPD experiments

The complexes of interest have been obtained as gaseous species by ESI of the above described solution prepared as described previously. Typical ESI conditions were a flow rate of 6 µL/min, a capillary spray voltage set at –5.0 kV, nebulizer at 12 PSI, drying gas flow at 5 L/min, and drying gas temperature at 275°C.

IRMPD experiments in the IR fingerprint range (900-1900 cm^{-1}) were recorded using the beamline of the IR free electron laser (FEL) of the Centre Laser Infrarouge

d'Orsay (CLIO). The FEL electron energy was set to 44 MeV to optimize the laser power in the frequency region of interest. The IR beam is allowed to interact with ion trapped in a hybrid FT-ICR tandem mass spectrometer (APEX-Qe Bruker) equipped with a 7.0 T actively shielded magnet and coupled to a quadrupole-hexapole interface for mass-filtering and ion accumulation.[55] Ions of interest were mass selected in the quadrupole and collisionally cooled for 300 ms in the hexapole with argon as buffer gas, prior to IR irradiation. Mass-selected complexes were irradiated for 0.2-0.5 s with the IR FEL light, after which the resulting mass spectrum was recorded. Laser attenuators were used in the case of the monodentate complex to avoid saturation and improve resolution of the most intense bands of its IRMPD spectrum.

IRMPD spectra are obtained by plotting the photofragmentation yield R ($R = -\ln[I_{parent}/(I_{parent} + \Sigma I_{fragment})]$), where I_{parent} and $I_{fragment}$ are the integrated intensities of the mass peaks of the precursor and of the fragment ions, respectively) as a function of the frequency of the IR radiation.[56]

2.3 Computational details

The most stable isomers and conformers of the *cis*-$[PtCl(NH_3)_2(CysGly)]^+$ and the *cis*-$[PtCl(NH_3)(CysGly)]^+$ complexes were identified by adopting the same computational procedure previously used [33] and briefly described as follows.

For each possible isomer a computational search was preliminary performed at the semiempirical tight-binding level, using the iMTD-GC approach implemented in CREST [57]. The resulting conformers were minimized at B3LYP/6-311+G(d,p) level of theory (using the LANL2DZ pseudopotential for Pt atom). A visual inspection was then performed in order to identify possible conformers that escaped the conformational sampling. For the surviving conformers a refinement of geometry,

electronic energies, thermodynamic properties (zero point energy (ZPE), thermal corrections, and entropies), and harmonic frequencies was obtained by minimizing the selected structures using a combined basis set, hereafter indicated as BS1, consisting of the 6–311+G(3df) basis set for the sulfur atom and 6–311+G(2df,pd) for the remaining atoms, except platinum, for which the LANL2TZ-f pseudopotential was adopted.

Harmonic frequencies computed for cis-$[PtCl(NH_3)_2(CysGly)]^+$ and *cis*-$[PtCl(NH_3)(CysGly)]^+$ complexes were scaled by 0.98. All the calculated spectra were convoluted assuming a Gaussian profile with an associated width (fwhm) of 15 cm^{-1}.

Considering the large number of conformers detected for each isomer, we reported in this work only the first ten lowest energy structures for each of them. The other structures, including the corresponding calculated IR spectra, are available upon request. All quantum chemical calculations were performed using the Gaussian 09 package [58].

For some specific structures (see results) of *cis*-$[PtCl(NH_3)(CysGly)]^+$ ion, we also performed fragment molecular orbital (FMO) calculations [59] with the three bodies approach (FMO3) [60] at RI-MP2/6-311G* level of theory [61,62]. The Pt atom was treated adopting the triple zeta model core potential (MCP-TZP) [63] and the electrostatic potential, described by the point-charges, was screened by using the damping function (SCREEN=1,1; RESPPC=-1) [64].The FMO method, associated with the pair interaction energy decomposition analysis (PIEDA) [65], has been widely applied to investigate macromolecular complexes such as protein-protein adducts [66,67], protein structures [68] and ligand-receptor complexes [69] also including metal-based binders [70]. Here, we used the FMO3/EDA approach [71] to study the *trans influence* exerted by SH on NH_3 and Cl^- ligands assessing the Pt-Cl

and Pt-NH_3 pair interaction energies (PIEs). PIE between two generic fragments, I and J, is defined as follows:

$$PIE^{IJ} = E^{IJ} - E^{I} - E^{J} + Tr(\Delta D^{IJ} V^{IJ}) \qquad (1)$$

where E^{IJ}, E^{I} and E^{J} are the internal energies of the IJ pair and of the isolated fragments I and J; ΔD^{IJ} is the density matrix difference between the dimer IJ and the monomers I and J electron densities and V^{IJ} is the matrix of the contribution of all other fragments to the electrostatic potential acting upon the dimer IJ [70].

The *cis*-$[PtCl(NH_3)(CysGly)]^+$ structures were split in four fragments: Pt^{2+}, Cys-Gly peptide, NH_3 and Cl^- ion. All FMO calculations were performed in gas phase by using the GAMESS-US suite (version: 30 june 2021 - R1) [72].

3. Results and discussions

3.1 Ionic products of the cisplatin-CysGly reaction

Cisplatin was incubated with the CysGly dipeptide in a water/methanol solution. The reaction products were analyzed using ESI-MS. The mass spectrum is presented in Figure S1. The presence of hydrolyzed cisplatin *cis*-$[PtCl(NH_3)_2(H_2O)]^+$ is confirmed by the cluster of ions at *m/z* 281-285 which shows the characteristic isotopic pattern of a Pt- and Cl-containing ion. In the presence of CysGly, substitution occurs at the expense of the water ligand, forming the monoadduct *cis*-$[PtCl(NH_3)_2(CysGly)]^+$ *m/z* 441-446. The spectrum also shows an isotopic cluster *m/z* 459-464 attributable to the non-covalent encounter complex of hydrolyzed cisplatin with CysGly, *cis*-$[PtCl(NH_3)_2(CysGly)(H_2O)]^+$, as already observed for the amino acids cysteine,[33] and methionine.[39] The isotopic cluster at *m/z* 424-428 can be attributed to the bidentate complex *cis*-$[PtCl(NH_3)(CysGly)]^+$, wherein an ammonia ligand was replaced by one of the nucleophilic functions of CysGly. This latter ion originates in

the gas-phase and can be observed in the ESI mass spectrum due to in-source fragmentation. Indeed, loss of ammonia is commonly observed in the CID of cisplatin-derived complexes [31-33,39-45,73] since ammonia acts as a better leaving group than chlorine in the absence of a protic solvent able to assist the substitution process. Moreover, the fragmentation path from *cis*-$[PtCl(NH_3)_2(L)]^+$ to *cis*-$[PtCl(NH_3)(L)]^+$, where L is a generic ligand, is facilitated in the case of chelating ligands due to the formation of a pentacoordinated transition state along the reaction coordinate, as reported in the case of the *cis*-$[PtCl(NH_3)_2(His)]^+$ complex [32]. For the sake of simplicity, in the forthcoming discussion ions containing Pt and Cl will be defined by the isotopic signal containing ^{194}Pt and ^{35}Cl, therefore we will refer to the ions at *m/z* 441 and *m/z* 424 to indicate *cis*-$[PtCl(NH_3)_2(CysGly)]^+$ and *cis*-$[PtCl(NH_3)(CysGly)]^+$, respectively.

3.2 IR ion spectra of cis-$[PtCl(NH_3)_2(CysGly)]^+$ *and cis*-$[PtCl(NH_3)(CysGly)]^+$

Complexes *cis*-$[PtCl(NH_3)_2(CysGly)]^+$ and *cis*-$[PtCl(NH_3)(CysGly)]^+$ were mass selected and irradiated in the 900 to 1900 cm^{-1} photon energy range. Photofragmentation mass spectra are reported in Figures S2 and S3 for *cis*-$[PtCl(NH_3)_2(CysGly)]^+$ and *cis*-$[PtCl(NH_3)(CysGly)]^+$, respectively. The former dissociates by ammonia loss producing the *m/z* 424 fragment ion. The subsequent dissociation channels are shared by both ions and consist of the competitive loss of either the second ammonia ligand or HCl, followed by the dissociation of the remaining ligand, thus generating a final fragment at *m/z* 371 assigned to $[Pt(CysGly)]^+$. The photodissociation yield (R) is plotted as a function of the photon wavenumber and reported in Figure 2. There is a clear similarity between the two spectra, which testifies that the complexes share similar binding motifs. In addition, the presence of absorptions above 1700 cm^{-1} indicates the existence of CO groups

which are not Pt bonded: the formation of a coordinative bond between C=O and Pt would lead to a reduction of the double bond strength with a significant red shift (below 1700 cm^{-1}) of the corresponding stretching mode. This evidence confirms the platinum preference for the S- and N-atoms of the thiol and amino functions in peptides.[29,33] For an accurate and extensive assignment of the IR absorption of the two ions, a theoretical investigation of the vibrational modes of their possible isomeric forms has been performed.

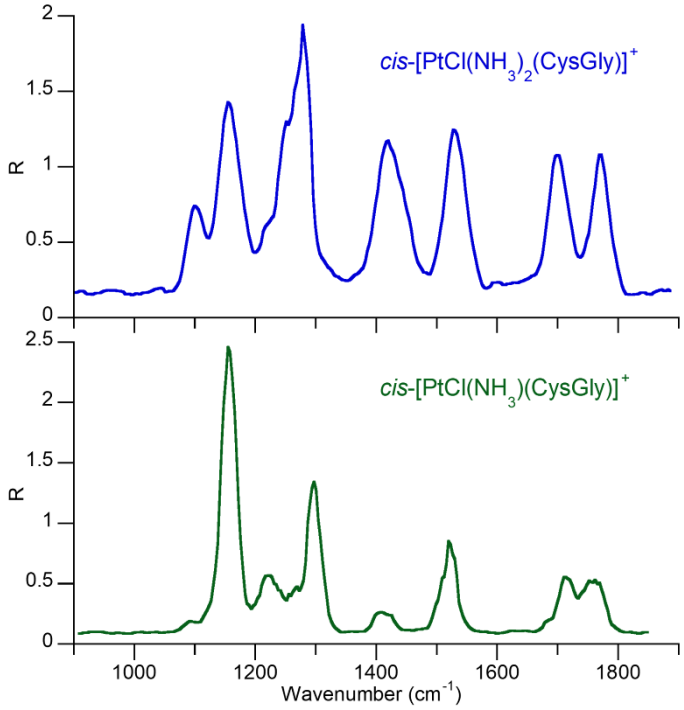

Figure 2. IRMPD spectra of *cis*-$[PtCl(NH_3)_2(CysGly)]^+$ (top) and *cis*-$[PtCl(NH_3)(CysGly)]^+$ (bottom).

3.3 Structure of the substitution product, cis-$[PtCl(NH_3)_2(CysGly)]^+$

When bound to a metal center, the CysGly dipeptide can act as monodentate as well as bidentate ligand. In the first case, the functional groups able to directly interact with Pt are -SH (Cys side chain), $-NH_2$ (Cys, peptide N-term), C=O (Cys, involved in peptide bond with Gly) and COOH (Gly, peptide C-term) leading to the

corresponding mono-adducts, hereafter indicated as cSH, cN, cCO and gCOOH, respectively, where the first letter represents the one letter code of the amino acid to which the group pertains (c for cysteine and g for glycine).

In the case of cSH and gCOOH isomers, the interaction with the Pt(II) ion increases the acidity of XH functions, thus promoting an intramolecular proton transfer to NH_2 or C=O moieties, and leading to the corresponding cS and gCOO isomers.

To identify the most stable isomers and conformers generated under the present experimental conditions, an extensive computational study was performed. The lowest energy structures obtained at the B3LYP/BS1 level of theory are shown in Figure 3 and the corresponding free energy values are reported in Table S1.

As found for the related complex *cis*-$[PtCl(NH_3)_2(Cys)]^+$ [33], cS is the most stable isomer, where the NH_3 function participates in three hydrogen bonds with Pt-bound S, O (peptide carbonyl moiety of cys) and Cl atoms. Indeed, the four lowest energy structures, **cS-1** - **cS-4**, share most of their intramolecular hydrogen bonds. Noteworthy, these H bond interactions coincide with those found for cis-$[PtCl(NH_3)_2(Cys)]^+$ (**cSz-1**, ref. 33) suggesting that the presence of glycine does not substantially affect the S-platination of cysteine. A different H bond pattern for the cS isomer has been found in **cS-7** (19.8 kJ mol^{-1}), where the protonated N-ter interacts with chlorine and cC=O while the carboxylic gC=O establishes a H bond with $(Pt)NH_3$ in *trans* position with respect to the Cl atom. The S atom is involved here in a H bond with the amidic NH function (Figure S4).

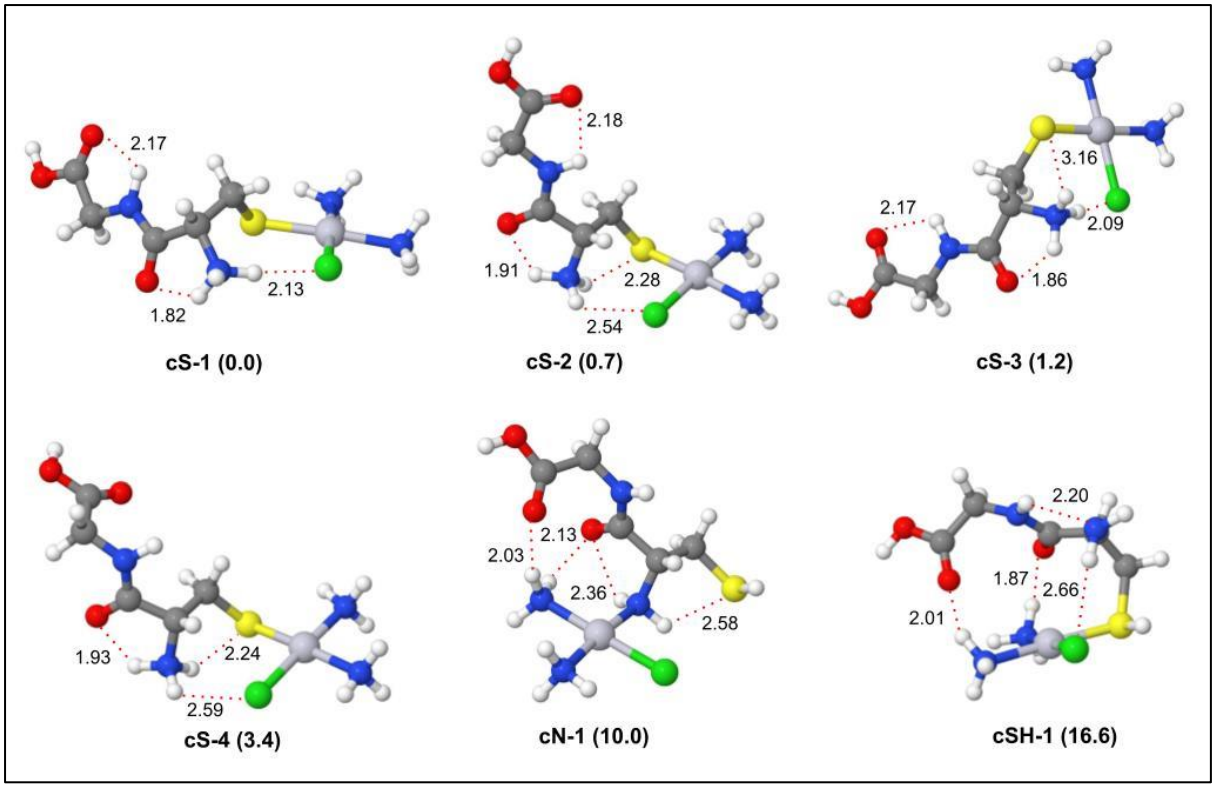

Figure 3. Optimized geometries of the most stable conformers of the *cis*-$[PtCl(NH_3)_2(CysGly)]^+$ ion computed in gas phase at B3LYP/BS1 level of theory. Free energies relative to **cS-1** are reported in parenthesis in kJ mol^{-1}. Hydrogen bond distances (Å) are indicated by a red dashed line.

When the thiol function is protonated, the relative energy rises to 16.6 kJ mol^{-1}, as shown by **cSH-1** isomer (Figure 3). In this structure, the C=O groups of cysteine and glycine interact via H bond with the two NH_3 ligands. Moreover, the lone pair of the NH_2 group is oriented to the opposite side of the Pt-bound SH function establishing a hydrogen bond with the amidic (N)H atom. Replacing the latter interaction with the formation of both SH···NH_2 and NH_2···Cl, achieved by rotation of the amino group, leads to an increase of relative free energy up to 27.5 kJ mol^{-1}, as reported for **cSH-2** (Figure S5). Notably, we also found a cSH conformer where NH_2 directly interacts with SH via a strong H bond with a length of 2.17 Å (**cSH-9**, Figure S5).

The lowest energy structure of the N-platinated product, **cN-1** (10.0 kJ mol^{-1}), is characterized by the cC=O engaged in two hydrogen bonds with Pt-NH_2 and (Pt)NH_3; the latter is also involved in a H bond with the C-term (CO moiety). The side chain of cysteine, containing the SH group, is oriented in the opposite direction of the peptide backbone forming the –S(H)···HNH(Pt) hydrogen bond. The remaining cN conformers are characterized by similar H bond patterns (Figure S4).

The carbonyl group of cysteine and glycine might also interact with the metal atom leading to the mono-substituted products cCO and gCOOH, respectively. **gCOOH-1** is slightly more stable than **cCO-1** with relative free energy of 61.9 and 65.8 kJ mol^{-1}, respectively (Figure S5).

In **gCOOH-1** the carboxylic OH is involved in a H bond with Cl while the NH_3 group, in *cis* position to C=O(Pt), interacts via H bonds with the -SH and C=O groups of cysteine. Finally, the NH_2 group establishes a H bond with the amidic NH, as found for cSH isomers.

The interaction with Pt increases the acidity of the COOH function and the most stable isomer of the gCOO family is only 4.5 kJ mol^{-1} higher in energy than the corresponding gCOOH isomer. In **gCOO-1**, the cC=O function is protonated and involved in a strong H bond with the free O atom of the COO moiety (H bond length of 1.37 Å). The proton released by the COOH moiety can also be transferred to the -NH_2 group, the most basic function of the molecule. However, the corresponding optimized conformers, **gCOO-6,** is 19.7 kJ mol^{-1} higher in energy indicating that the positive charge is stabilized more efficiently when the protonation site is the C=O function of cysteine.

In the other gCOOH conformers (**gCOOH-2**, **gCOOH-3** and **gCOOH-4**) the COOH moiety assumes a *trans* configuration, with OH interacting with the amidic C=O group (Figures S5 and S6).

When the CysGly dipeptide binds Pt via cC=O, the most stable conformer **cCO-1** is characterized by several H bonds between NH and NH_2 and between the SH and CO(OH) as acceptors with a NH_3(Pt) ligand (Figure S5). In the remaining cCO conformers the other H bond donor/acceptor functional groups, such as SH, COOH and NH_2, are free to give rise to different H bond patterns as shown in Figure S6.

3.4 Spectral assignment of the cis-$[PtCl(NH_3)_2(CysGly)]^+$ *IRMPD spectrum*

The IRMPD spectrum of *cis*-$[PtCl(NH_3)_2(CysGly)]^+$ was compared with the calculated IR spectra of the isomers and conformers obtained from the exploration of the ion conformational space. Figure 4 displays the experimental spectrum superimposed on the theoretical harmonic spectra of the four most stable S-bound conformers (**cS-1, cS-2, cS-3, cS-4**) and the lowest energy conformers pertaining to the isomeric families either N-bound or SH-bound, **cN-1** and **cSH-1**, respectively. At first glance, the spectra clearly show that the experiment is very well simulated by the IR frequencies of the **cS-1**-**4** complexes (Table S2), which share a similar profile. The two bands in the highest wavenumber range of the fingerprint spectrum are well interpreted by the CO stretching modes of the cysteine and glycine residues calculated for all the reported **cS** isomers at ca. 1700 and 1770 cm^1, respectively. The calculated NH bend of the amidic group is in good agreement with the IRMPD band at 1530 cm^{-1}, while the following band at 1420 cm^{-1} can be assigned to vibrational modes involving the umbrella motion of the protonated amino group of cysteine and the OH bend of glycine, which fall in the 1400-1450 cm^{-1} range for **cS-1**-**4**. The most intense signal of the IRMPD spectrum at 1286 cm^{-1} is related to the

umbrella modes of the ammonia ligands of platinum, while the 1155 cm^{-1} experimental band is well reproduced by the OH bend of glycine carboxylic group. Finally, the 1113 cm^{-1} signal is a combination of the NC stretch in glycine with combined NH and CH bending modes of the CysGly cysteine residue.

Isomer **cN-1**, with a relative free energy of 10.0 kJ mol^{-1} could explain some of the experimental absorptions; however, its profile presents hardly any vibrational activity around 1420 cm^{-1}, and at 1100 cm^{-1}, unlike the IRMPD spectrum. Moreover, the CO stretch of cysteine in CysGly is calculated at 1659 cm^{-1}, showing poor agreement with the experimental band at 1705 cm^{-1}. The theoretical spectrum of **cSH-1**, with relative free energy of 16.6 kJ mol^{-1}, presents the same limitations. A detailed description of the vibrational modes of **cN-1** and **cSH-1** is reported in Table S3 and Table S4, respectively.

Considering their high relative free energies, we expect that the gCOOH, cCO, and gCOO isomers do not contribute to the experimental IRMPD spectrum. As shown in Figure 4, this is confirmed by the poor correspondence between experimental data and theoretical IR absorptions computed for their low-lying structures, **gCOOH-1**, **cCO-1** and **gCOO-1**. Notably, the cC=O and gC=O stretching modes are predicted below 1700 cm^{-1} due to coordination with the Pt atom (Table S5).

Comparison between experimental IRMPD spectrum and theoretical IR signatures of the remaining *cis*-$[PtCl(NH_3)_2(CysGly)]^+$ isomers and conformers are shown in Figures S7-S10.

Overall, based on both spectroscopic and thermodynamic data, it is possible to confirm the preference for platinum to bind the deprotonated thiolic group of cysteine even when interacting with a more complex bio-ligand, such as the present CysGly dipeptide.

As a side note, we point out that IRMPD spectroscopy coupled with QM calculations can unambiguously assess the cis/trans isomerism of the peptide bond [73-76]. Notably, although the most stable configuration of the peptide bond is the *trans* geometry, a small but relevant percentage of the peptide bonds has been found in *cis* configuration [77, 49]. Therefore, an explorative computational study starting from the lowest energy isomer, **cS-1**, was performed to assess whether platination might affect the peptide bond configuration. As shown in Figure 5, the ***cis* cS-1** isomer was found to lie 29.8 kJ mol^{-1} higher in energy than the corresponding *trans* structure (the global minimum), highlighting that the *trans* configuration of the peptide bond is the most stable also in the presence of Pt(II) coordination of CysGly. This result is confirmed by comparison of the ***cis* cS-1** theoretical IR signatures with the IRMPD spectrum (Figure 5). In fact, its computed IR spectrum is characterized by the absence of the relevant band at 1530 cm^{-1} because this absorption, associated to bending mode of the amidic N-H function coupled with CO-NH stretch, is significantly red shifted (1403 cm^{-1}) as consequence of the steric clashes between the two moieties in trans positions which also induce a slight elongation of the peptide bond (Figure 5). In ***cis* cS-1,** the amidic N-H bending mode is also coupled with cC=O stretch, predicted at 1707 cm^{-1}.

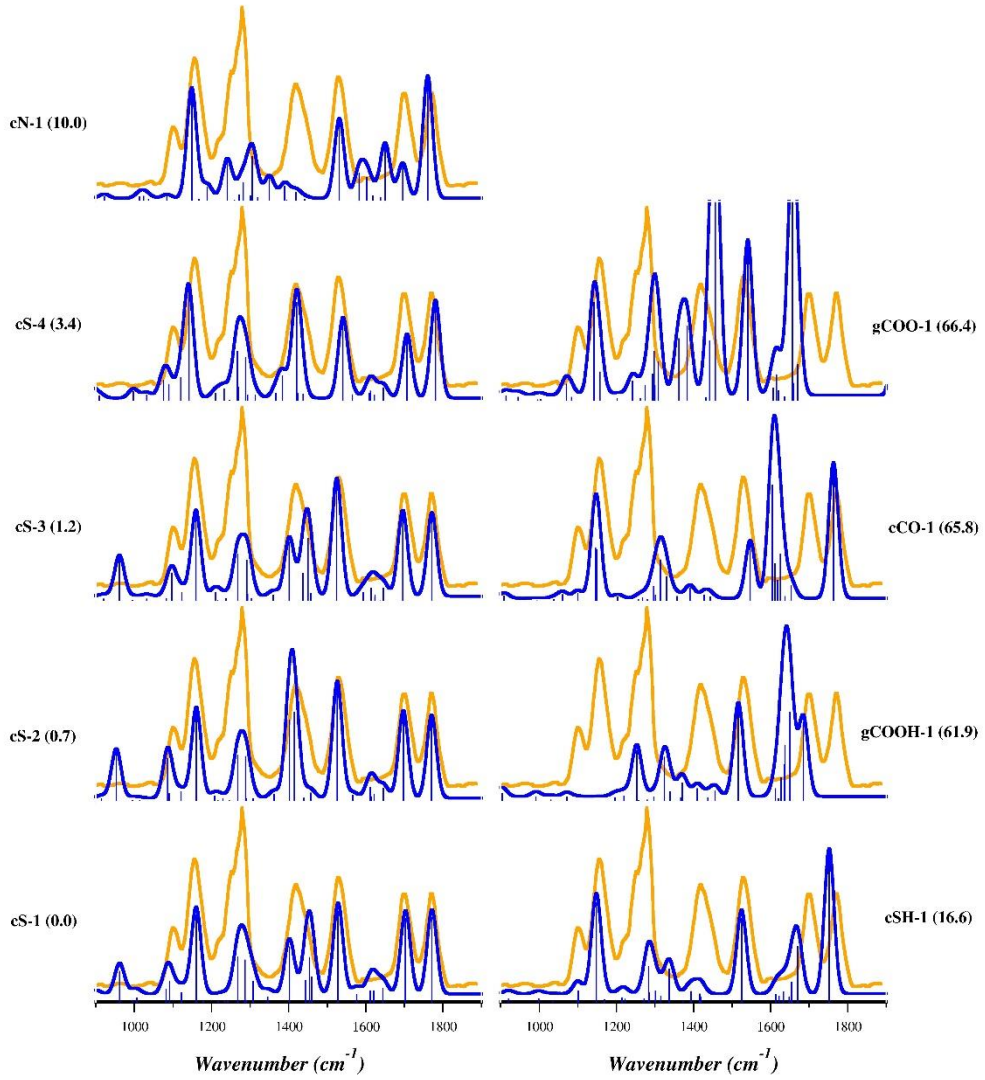

Figure 4. IRMPD spectrum (orange profile) and calculated harmonic IR spectra (blue profiles) of the lowest lying conformers and isomers of *cis*-$[PtCl(NH_3)_2(CysGly)]^+$ ion (blue profile), computed at the B3LYP/BS1 level of theory. Free energies relative to **cS-1** are reported in brackets (kJ mol^{-1}).

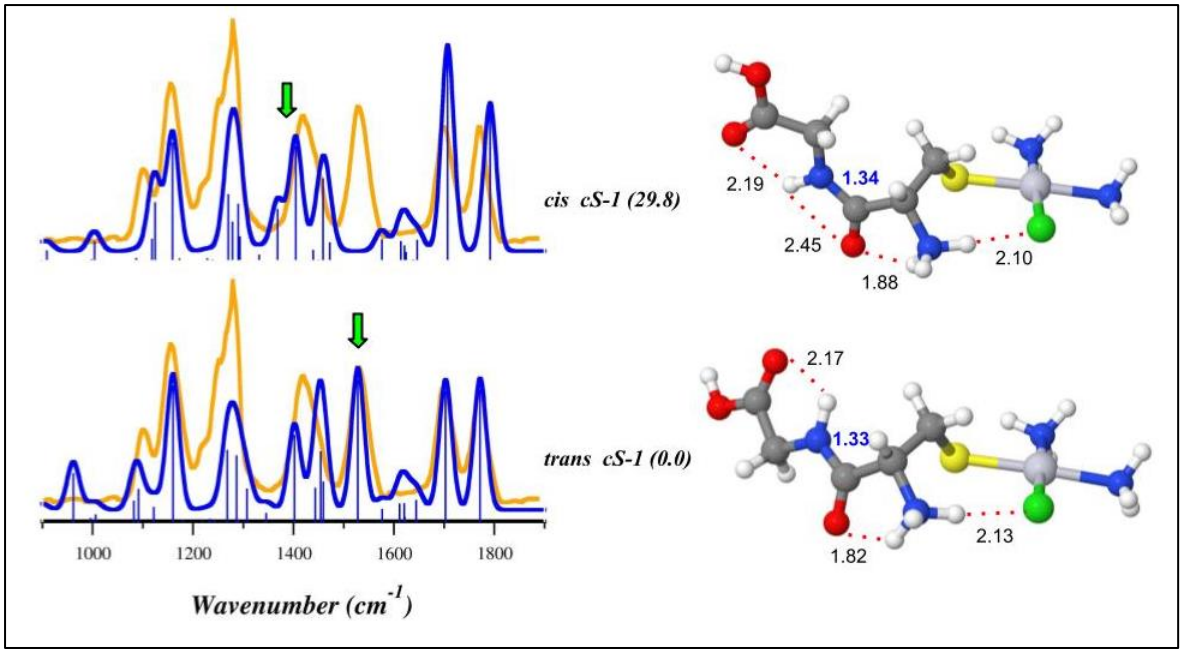

Figure 5. IRMPD spectrum (orange profile), calculated harmonic IR spectra (blue profiles) and optimized geometries of the lowest energy structures of the *cis* and *trans* CysGly peptide isomers (***cis cS-1*** and ***trans cS-1***, respectively) of *cis*-$[PtCl(NH_3)_2(CysGly)]^+$ ion (blue profile), computed at the B3LYP/BS1 level of theory. Lengths (in Å) of the peptide bonds are reported in blue. Free energies relative to **cS-1** are reported in brackets (kJ mol^{-1}). The vibrational band associated with amidic N-H bending mode coupled with CO-NH stretch is highlighted by a green arrow.

3.5 Structure of the chelation product cis-$[PtCl(NH_3)(CysGly)]^+$

The dipeptide CysGly is characterized by four nucleophilic groups and therefore it can act as a bidentate ligand. After the first substitution, *cis*-$[PtCl(NH_3)_2(CysGly)]^+$ can undergo a second substitution event by replacement of one amino ligand, leading to the chelation product, *cis*-$[PtCl(NH_3)(CysGly)]^+$. Starting from the first substitution complexes - cS, cSH, cN, cO, gCOOH and gCOO - several chelation isomers can be obtained, depending on the second nucleophilic group that binds Pt and hereafter indicated as **cS_cN-n**, **cSH_cN-n**, **cN_cS-n** and so on, in which the

first and second groups indicates those in trans to the ammonia and to the Cl ligands, respectively.

Geometry optimization and frequency calculations were performed to identify the lowest energy isomers and conformers in the gas phase. The corresponding free energy values are reported in Table S6.

As shown in Figure 6, the most stable isomer is represented by the chelation product **cN_cSH-1**, obtained from a cN isomer after a second substitution performed by SH moiety. The structure is characterized by an open conformation, similar to that of **cS-1**, where the glycine is stretched out in an opposite direction relative to Pt. Indeed, only two hydrogen bonds are established between the cC=O and NH_2(Pt) and between the C=O and NH of glycine. As shown by **cN_cSH-2** (Figure 6), a "folded conformation" can be obtained after epimerization of S atom. Due to S-metalation, the latter becomes the second chiral center (the first being the C_α atom of cysteine with R configuration) of the complex assuming S or R configuration. In **cN_cSH-1** (R, R), the hydrogen atom of the S-H function – with R configuration – is oriented toward the bottom of the Cl-Pt-NH_3 plane and therefore it cannot establish a H bond with the carboxylic function of glycine. On the contrary, in the **cN_cSH-2** (R, S) structure, the H atom bound to sulfur in S configuration is oriented above the Pt–containing plane allowing a strong H bond interaction of S-H with gC=O. Furthermore, the H bond between cC=O and NH_2(Pt) becomes shorter, changing from 2.15 to 2.04 Å.

The **cSH_cN-1** (R, S) isomer is 21.2 kJ mol^{-1} higher in energy than **cN_cSH-1** (R, R) indicating that the cN_cSH configuration is more stable than cSH_cN, in agreement with previous results obtained for *cis*-$[PtCl(NH_3)(Cys)]^+$.[33]

Interestingly, **cSH_cN-1** (R, S) has the same "folded conformation" found for **cN_cSH-2** (R, S) while **cSH_cN-2** (R, R) and **cN_cSH-1** (R, R) have a stretched

conformation. Therefore, the R,R configuration is the most stable one for the cN_cSH isomer while R,S is the lowest energy configuration for the cSH_cN isomer. Notably, the cN_SH and cSH_cN geometrical isomers only differ for the position of Cl and NH_3 ligands. In cN_cSH the Cl and NH_3 ligands are in *trans* and *cis* position to SH, respectively, while an opposite configuration characterizes the cSH_cN isomers. The different stability of the R,R and R,S epimers (stretched/folded conformation) for the two low-lying geometrical isomers can therefore be reasonably attributed to the slight modulation of the *trans* influence [78] of the thiol moiety due to H bond formation.

The PIE analysis indicates that the formation of a H bond between SH and cC=O in **cN_cSH-2** reduces the Pt-Cl interaction energy by 2.9 kcal mol^{-1} while no impact on Pt-NH_3 binding strength has been found (Table S7). As a result, **cN_cSH-2** is a less stable structure than **cN_cSH-1.** Conversely, as shown in Table S8, in **cSH_cN-1** and **cSH_cN-2** the Pt-Cl and Pt-NH_3 PIE values are comparable, with total ΔPIE of –0.2 kcal mol^{-1}, suggesting that the ligand in *trans* position to SH, the neutral NH_3, is less affected by the increased *trans* influence of S than the negatively charged chlorido ligand. As a consequence, the formation of the strong SH···CO hydrogen bond in **cSH_cN-1** stabilizes the structure more than the weak destabilization of the Pt-NH_3 bond due to the increased trans influence of SH moiety, when it is engaged in H bond. Other possible chelation products are the cN_cCO and cSH_cCO isomers. The lowest energy structures of these families are **cN_cCO-1** and **cSH_cCO-1** at 31.1 and 38.1 kJ mol^{-1} relative free energy, respectively (Figure S11). Starting from the latter, the proton transfer from the SH(Pt) function to cC=O leads to **cS_cCO-1** isomer, with a significant increase of relative free energy (84.2 kJ mol^{-1}).

We also explored the stability of the cN_gN, cSH_gN and cS_gN isomers (Figure S12). The low-lying isomer is represented by **cN_gN-1** (75.3 kJ mol^{-1}) where the deprotonated amidic N atom chelates the Pt with protonation of cC=O. If the N-H function retains the proton, the relative free energy increases up to 95.6 kJ mol-1 (**cN_gN-2**, Figure S12).

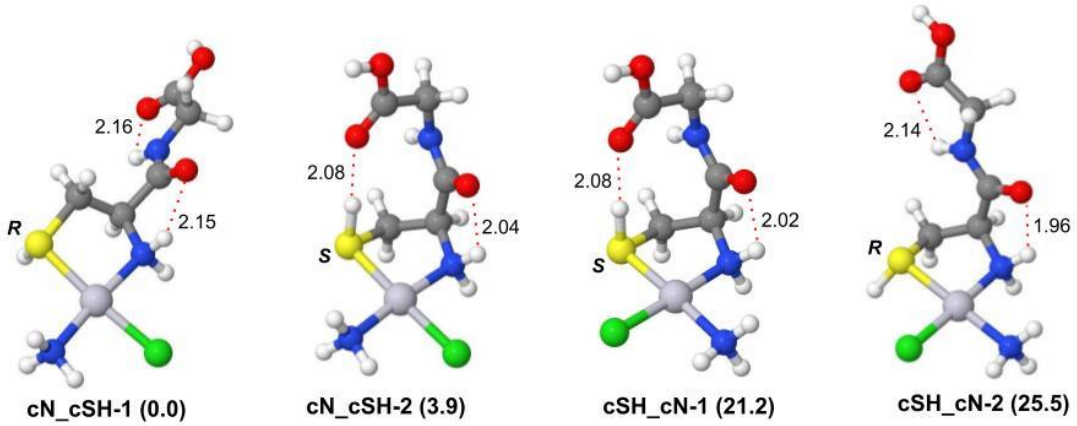

Figure 6. Optimized geometries of the most stable conformers of the cis-$[PtCl(NH_3)(CysGly)]^+$ ion, computed in gas phase at B3LYP/BS1 level of theory. Free energies relative to **cN_cSH-1** are reported in parenthesis in kJ mol^{-1}. Hydrogen bond distances (Å) are indicated by a red dashed line. The configuration of S* atom is also shown (R or S).

3.6 Reaction pathway of the chelation process.

The bi-dentate complex, *cis*-$[PtCl(NH_3)(CysGly)]^+$, is obtained in the gas-phase by in-source fragmentation of the isolated mono-dentate adduct, *cis*-$[PtCl(NH_3)_2(CysGly)]^+$. As described previously, the predominant *cis*-$[PtCl(NH_3)_2(CysGly)]^+$ isomer in the sampled ion population is the cS isomer. Accordingly, the most abundant chelation product can be identified in the corresponding cSH_cN isomer. The reaction pathway of this process is composed by two steps: *i*) cS → cSH and *ii*) cSH → cSH_cN. The first step consists of an intramolecular proton transfer from NH_3^+ to S(Pt). Based on

the barrier calculated for a similar process involving the *cis*-[PtCl(NH_3)$_2$(Cys)]$^+$ complex, an energy barrier of about 39 kJ mol^{-1} can be hypothesized.[33] The second step occurs via an intramolecular SN_2-like mechanism where the NH_2 function attacks the Pt atom with release of the NH_3 moiety (leaving group). The corresponding transition state (TS) is characterized by the well-known pentacoordinated adduct (Figure S13) where the bond angle NH_2-Pt-NH_3 is 76.4° (typically < 80°). Intrinsic reaction coordinate (IRC) calculations confirm this TS structure (Figure S14) which presents an energy barrier of 113.8 kJ mol^{-1} (Figure S15), indicating that the latter step is the rate-limiting step of the cS → cSH_cN chelation reaction.

In addition, we investigated reaction pathways of alternative chelation processes in which the cN isomer of the mono-adduct complex is the starting point. This reaction is characterized by one step, cN → cSH_cN, where the free SH moiety attacks the Pt atom forming a bond angle SH-Pt-NH_3 of 79.4°. The TS structure (Figure S16) has been confirmed by IRC calculations (Figures S17) and presents a relative free energy of 108.6 kJ mol^{-1} (Figure S15). Comparison of the energy barriers of the two processes, indicates that there are no significant differences between the kinetics of the two chelation reactions.

3.7 Spectral assignment of the cis-[PtCl(NH_3)(CysGly)]$^+$ IRMPD spectrum

Figure 7 compares the experimental IRMPD spectrum of *cis*-[PtCl(NH_3)(CysGly)]$^+$ (red profile) with the calculated vibrational spectra of the lowest energy conformers of the isomeric families cN_cSH, cSH_cN, cN_cCO, cSH_cCO and cN_gN**.** Theoretical IR spectra of other *cis*-[PtCl(NH_3)(CysGly)]$^+$ isomers and conformers are shown in Figures S18 and S19.

The *cis*-[PtCl(NH_3)(CysGly)]$^+$ IRMPD spectrum shows similarities with the spectrum of the monodentate complex as evident from the comparison of the two spectra presented in Figure 2. This indication agrees with the hypothesis that the chelate ion is produced by fragmentation of *cis*-[PtCl(NH_3)$_2$(CysGly)]$^+$ inside the mass spectrometer, thus presenting similar binding motifs. The lowest lying structure, **cN_cSH_1** and its isomer **cN_cSH_2**, can both interpret the experiment quite well, however these isomers may only be generated by chelation starting from a cN isomer of *cis*-[PtCl(NH_3)$_2$(CysGly)]$^+$, a species which is not present in the assayed ionic population as discussed in the previous section. On the other hand, **cSH_cN_1** and **cSH_cN_2** perfectly match the IRMPD spectrum as shown in Figure 7 and represent the lowest energy isomers produced by chelation from the cS isomer of *cis*-[PtCl(NH_3)$_2$(CysGly)]$^+$, predominant in this ionic population.

A detailed description of mode assignment is reported in Tables S9 and S10. Among the spectroscopic features, it is interesting to compare the CO stretching signals of the chelate with the ones of the monodentate. In the chelate complex, bands at 1717 and 1768 cm^{-1}, attributed to CO stretching modes of cysteine and glycine, respectively, are closer in frequency than the correspondng bands in cis-[PtCl(NH_3)$_2$(CysGly)]$^+$ by ca. 20 cm^{-1}. Calculations reproduce this feature well. Arguably, the cysteine CO stretching mode is slightly more red-shifted in the monodentate complex due to the interaction with a stronger H-bond donor, the hydrogen of the protonated amino group, when compared to the hydrogen of the amino group bound to platinum in the chelate ion. It is worth pointing out the absence of any strong absorption around 1450 cm^{-1}. This band was assigned to the monodentate complex to the umbrella mode of the protonated amino group of

cysteine. Its absence is a clear indication of the binding of the same amino group to platinum in the *cis*-[PtCl(NH_3)(CysGly)]$^+$ complex.

Both the relative free energy values and the comparison between experimental and theoretical spectra (Figure 7 and Table S10) clearly indicate that the second nucleophilic group involved in the chelation reaction cannot be associated with the cCO (**cN_cCO-1** and **cSH_cCO-1**) or to the amidic NH (**cN_gN-1**) functions.

Spectroscopic data finally assess the formation of a chelate complex **cSH_cN** which is in line with reported findings in the case of the cisplatin-methionine interaction.[39]

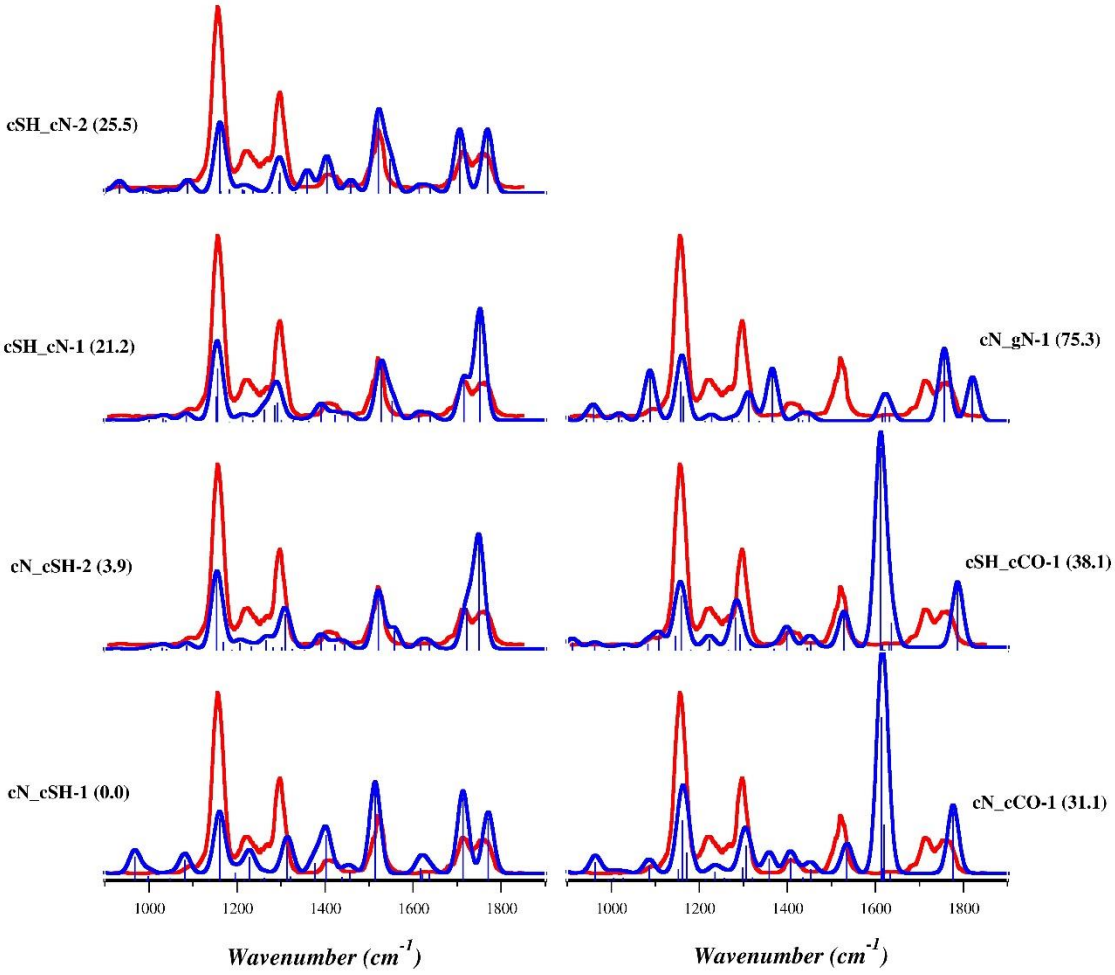

Figure 7. IRMPD spectrum (red profile) and calculated harmonic IR spectra of the lowest lying isomers and conformers of *cis*-[PtCl(NH_3)(CysGly)]$^+$ ion (blue profile),

computed at the B3LYP/BS1 level of theory. Free energies relative to **cN_cSH-1** are reported in brackets (kJ mol^{-1}).

4. Conclusions

In this work, we report IRMPD experiments combined with DFT calculations to characterize the products of mono-substitution and of the subsequent chelation reactions of cisplatin with the CysGly dipeptide, selected as functional model of GSH.

We found that the IRMPD spectrum of *cis*-$[PtCl(NH_3)_2(CysGly)]^+$ in the IR fingerprint range (900-1900 cm^{-1}) is satisfactorily reproduced by the theoretical harmonic spectra of the lowest energy S-bound conformers, showing the same H bond pattern of *cis*-$[PtCl(NH_3)_2(Cys)]^+$, as previously reported. The vibrational band at 1420 cm^{-1} attributed to the umbrella mode of the protonated amino group of cysteine is highly diagnostic since it is not present in N-bound isomer allowing an unambiguous attribution. This evidence indicates that the thiol function is the most favorite metalation site of the CysGly dipeptide. Moreover, the combination of IRMPD spectroscopy with DFT calculations allowed us to study the possible impact of the reaction with cisplatin on the peptide bond configuration. The findings showed that the trans dipeptide remains the most stable CysGly isomer even after the platination process.

The chelation product, *cis*-$[PtCl(NH_3)(CysGly)]^+$, has been obtained by means of fragmentation of *cis*-$[PtCl(NH_3)_2(CysGly)]^+$ inside the mass spectrometer. Therefore, it is presumably originated from conformers of the lowest energy S-bound isomer, after chelation engaging the alpha amino group of cysteine. Indeed, the corresponding IRMPD spectrum is well interpreted by conformers of the S,N-bound

epimers, whose most stable structure is characterized by an intramolecular H bond between the CO and SH groups of cysteine, allowed only with sulfur in S configuration.

The results reported herein may contribute to extend the information about the cisplatin reactivity with biological thiol derivatives, useful for an in depth understanding of the cisplatin resistance mechanism associated to GSH and eventually to design more effective Pt-based anticancer drugs.

Acknowledgements

This work has been funded by the Università degli Studi di Roma La Sapienza.

We are grateful to Philippe Maître and Debora Scuderi and the CLIO team. Financial Support from the French National FT-ICR network (No. FR3624 CNRS) for conducting the research is gratefully acknowledged.

References

[1] Cisplatin: Chemistry and Biochemistry of a Leading Anticancer Drug; Lippert, B., Ed.; Wiley, 1999.

[2] E.R. Jamieson, S.J. Lippard, Structure, Recognition, and Processing of Cisplatin−DNA Adducts, Chem. Rev. 99 (1999) 2467− 2498,

[3] E. Wong, C.M. Giandomenico, Current Status of Platinum- Based Antitumor Drugs, Chem. Rev. 99 (1999) 2451−2466, https://doi.org/10.1021/cr980420v .

[4] M.A. Fuertes, C. Alonso, J.M. Pérez, Biochemical Modulation of Cisplatin Mechanisms of Action: Enhancement of Antitumor Activity and Circumvention of Drug Resistance, Chem. Rev. 103 (2003) 645−662, https://doi.org/10.1021/cr020010d.

[5] A.V. Klein, T.W. Hambley, Platinum Drug Distribution in Cancer Cells and Tumors, Chem. Rev. 109 (2009) 4911−4920, https://doi.org/10.1021/cr9001066

[6] S. Dasari, P.B. Tchounwou, Cisplatin in Cancer Therapy: Molecular Mechanisms of Action, Eur. J. Pharmacol. 740 (2014) 364− 378, https://doi.org/10.1016/j.ejphar.2014.07.025 .

[7] P. J. Loehrer, L. H. Einhorn, Drugs 5 Years Later – Cisplatin, Ann. Intern. Med. 100 (1984) 704-713.

[8] C. Bokemeyer, H.J. Schmoll, A. Harstrick, Side-effects of GM-CSF treatment in Advanced Testicular Cancer, Eur. J. Cancer 29A (1993) 924-924.

[9] T. L. Cornelison, E. Reed, Nephrotoxicity and Hydration Management for Cisplatin, Carboplatin, and Ormaplatin, Gynecol. Oncol. 50 (1993) 147-158.

[10] M. Kartalou, J. M. Essigmann, Mechanisms of resistance to cisplatin, Mutat. Res. 478 (2001) 23-43.

[11] T. C. Johnstone, K. Suntharalingam, S. J. Lippard, The Next Generation of Platinum Drugs: Targeted Pt(II) Agents, Nanoparticle Delivery, and Pt(IV) Prodrugs, Chem. Rev. 116 (2016) 3436-3486.

[12] R.P. Perez, Cellular and molecular determinants of cisplatin resistance, Eur. J. Cancer. 34 (1998) 1535–1542. doi:10.1016/S0959-8049(98)00227-5.

[13] S.H. Chen, J.Y. Chang, New insights into mechanisms of cisplatin resistance: From tumor cell to microenvironment, Int. J. Mol. Sci. 20 (2019). doi:10.3390/ijms20174136.

[14] T. Minervini, B. Cardey, S. Foley, C. Ramseyer, M. Enescu, Fate of cisplatin and its main hydrolysed forms in the presence of thiolates: A comprehensive computational and experimental study, Metallomics. 11 (2019) 833–844. doi:10.1039/c8mt00371h.

[15] A. Eastman, Cross-linking of glutathione to DNA by cancer chemotherapeutic platinum coordination complexes, Chem. Biol. Interact. 61 (1987) 241–248. doi:10.1016/0009-2797(87)90004-4.

[16] T.G. Appleton, J.W. Connor, J.R. Hall, P.D. Prenzler, NMR Study of the reactions of the cis-diamminediaquaplatinum(II) cation with glutathione and amino acids containing a thiol group, Inorg. Chem. 28 (1989) 2030–2037. doi:10.1021/ic00310a007.

[17] H. HW Chen, M. Tien Kuo, Role of glutathione in the regulation of Cisplatin resistance in cancer chemotherapy. Metal-based drugs, 2010 (2010) 1-7. doi:10.1155/2010/430939

[18] A. Casini, J. Reedijk, Interactions of Anticancer Pt Compounds with Proteins: An Overlooked Topic in Medicinal Inorganic Chemistry? Chem. Sci. 3 (2012) 3135, https://doi.org/10.1039/C2SC20627G.

[19] L. Messori, A. Merlino, Cisplatin Binding to Proteins: Molecular Structure of the Ribonuclease A Adduct, Inorg. Chem. 53 (2014) 3929−3931, https://doi.org/10.1021/ic500360f.

[20] A.I. Ivanov, J. Christodoulou, J.A. Parkinson, K.J. Barnham, A. Tucker, J. Woodrow, P.J. Sadler, Cisplatin Binding Sites on Human Albumin, J. Biol. Chem. 273 (1998) 14721−14730, https://doi.org/10.1074/jbc.273.24.14721.

[21] H. Li, Y. Zhao, H.I.A. Phillips, Y. Qi, T.Y. Lin, P.J. Sadler, P.B. O'Connor, Mass Spectrometry Evidence for Cisplatin as a Protein Cross-Linking Reagent, Anal. Chem. 83 (2011) 5369−5376, https://doi.org/10.1021/ac200861k.

[22] F. Arnesano, S. Scintilla, G. Natile, Interaction between Platinum Complexes and a Methionine Motif Found in Copper Transport Proteins, Angew. Chem., Int. Ed. 46 (2007) 9062−9064, https://doi.org/10.1002/ange.200703271.

[23] C.M. Sze, G.N. Khairallah, Z. Xiao, P.S. Donnelly, R.A.J. O'Hair, A.G. Wedd, Interaction of Cisplatin and Analogues with a Met-Rich Protein Site, J. Biol. Inorg. Chem. 14 (2009) 163−165, https://doi.org/10.1007/s00775-008-0452-x.

[24] H. Li, J.R. Snelling, M.P. Barrow, J.H. Scrivens, P.J. Sadler, P.B. O'Connor, Mass Spectrometric Strategies to Improve the Identification of Pt(II)-Modification Sites on Peptides and Proteins, J. Am. Soc. Mass Spectrom. 25 (2014) 1217−1227, https://doi.org/10.1007/s13361-014-0877-0.

[25] C.M. Sze, G.N. Khairallah, Z. Xiao, P.S. Donnelly, R.A.J. O'Hair, A.G. Wedd, Interaction of cisplatin and analogues with a Met-rich protein site, JBIC J. Biol. Inorg. Chem. 14 (2009) 163–165. doi:10.1007/s00775-008-0452-x.

[26] L. Feketeová, V. Ryzhov, R.A.J. O'Hair, Comparison of collision- versus electron-induced dissociation of Pt(II) ternary complexes of histidine- and methionine-containing peptides, Rapid Commun. Mass Spectrom. 23 (2009) 3133–3143. doi:10.1002/rcm.4234.

[27] Ž.D. Bugarčić, J. Bogojeski, B. Petrović, S. Hochreuther, R. van Eldik, Mechanistic Studies on the Reactions of Platinum(II) Complexes with Nitrogen- and Sulfur-Donor Biomolecules, Dalton Trans. 41 (2012) 12329, https://doi.org/10.1039/C2DT31045G

[28] V. Saudek, H. Pivcova, D. Noskova, J. Drobnik, The Reaction of Pt-Antitumor Drugs with Selected Nucleophiles .2. Preparation and Characterization of Coordination-Compounds of Pt(II) and L-Histidine, J. Inorg. Biochem. 23 (1985) 55-72.

[29] T. G. Appleton, Donor Atom Preferences in Complexes of Platinum and Palladium with Amino Acids and Related Molecules, Coord. Chem. Rev. 166 (1997) 313-359.

[30] T.G. Appleton, J.W. Connor, J.R. Hall, S,O- versus S,N-chelation in the reactions of the cis-diamminediaquaplatinum(II) cation with methionine and S-methylcysteine, Inorg. Chem. 27 (1988) 130–137. doi:10.1021/ic00274a027.

[31] R. Paciotti, D. Corinti, A. De Petris, A. Ciavardini, S. Piccirillo, C. Coletti, N. Re, P. Maitre, B. Bellina, P. Barran, B. Chiavarino, M. Elisa Crestoni, S. Fornarini, Cisplatin and transplatin interaction with methionine: bonding motifs assayed by vibrational spectroscopy in the isolated ionic complexes, Phys. Chem. Chem. Phys. 19 (2017) 26697–26707. doi:10.1039/C7CP05203K.

[32] D. Corinti, A. De Petris, C. Coletti, N. Re, B. Chiavarino, M.E. Crestoni, S. Fornarini, Cisplatin Primary Complex with l-Histidine Target Revealed by IR Multiple Photon Dissociation (IRMPD) Spectroscopy, ChemPhysChem. 18 (2017) 318–325. doi:10.1002/cphc.201601172.

[33] D. Corinti, R. Paciotti, C. Coletti, N. Re, B. Chiavarino, M.E. Crestoni, S. Fornarini, Elusive intermediates in cisplatin reaction with target amino acids: Platinum(II)-cysteine complexes assayed by IR ion spectroscopy and DFT calculations, J. Inorg. Biochem. 237 (2022) 112017. doi:10.1016/j.jinorgbio.2022.112017.

[34] L. MacAleese, P. Maître, Infrared Spectroscopy of Organo-metallic Ions in the Gas Phase: From Model to Real World Complexes, Mass Spectrom. Rev. 26 (2007) 583−605, https://doi.org/10.1002/mas.20138.

[35] L. Jašíková, J. Roithová, Infrared Multiphoton Dissociation Spectroscopy with Free-Electron Lasers: On the Road from Small Molecules to Biomolecules, Chem. - Eur. J. 24 (2018) 3374−3390, https://doi.org/10.1002/chem.201705692.

[36] J.R. Eyler, Infrared Multiple Photon Dissociation Spectroscopy of Ions in Penning Traps. Mass Spectrom. Rev. 28 (2009) 448−467, https://doi.org/10.1002/mas.20217.

[37] T.D. Fridgen, Infrared Consequence Spectroscopy of Gaseous Protonated and Metal Ion Cationized Complexes. Mass Spectrom. Rev. 28 (2009) 586−607, https://doi.org/10.1002/mas.20224.

[38] N.C. Polfer, J. Oomens, Vibrational Spectroscopy of Bare and Solvated Ionic Complexes of Biological Relevance, Mass Spectrom. Rev. 28 (2009) 468−494, https://doi.org/10.1002/mas.20215.

[39] R. Paciotti, D. Corinti, P. Maitre, C. Coletti, N. Re, B. Chiavarino, M.E. Crestoni, S. Fornarini, From Preassociation to Chelation: A Survey of Cisplatin Interaction with Methionine at Molecular Level by IR Ion Spectroscopy and Computations, J. Am. Soc. Mass Spectrom. 32 (2021) 2206–2217. doi:10.1021/jasms.1c00152.

[40] D. Corinti, M.E. Crestoni, B. Chiavarino, S. Fornarini, D. Scuderi, J.-Y. Salpin, Insights into Cisplatin Binding to Uracil and Thiouracils from IRMPD Spectroscopy and Tandem Mass Spectrometry, J. Am. Soc. Mass Spectrom. 31 (2020) 946–960. doi:10.1021/jasms.0c00006.

[41] B. Chiavarino, M.E. Crestoni, S. Fornarini, D. Scuderi, J.-Y.Y. Salpin, Interaction of Cisplatin with Adenine and Guanine: A Combined IRMPD, MS/MS, and Theoretical Study, J. Am. Chem. Soc. 135 (2013) 1445–1455. doi:10.1021/ja309857d.

[42] B. Chiavarino, M.E. Crestoni, S. Fornarini, D. Scuderi, J.-Y. Salpin, Interaction of Cisplatin with 5′-dGMP: A Combined IRMPD and Theoretical Study, Inorg. Chem. 54 (2015) 3513–3522. doi:10.1021/acs.inorgchem.5b00070.

[43] B. Chiavarino, M.E. Crestoni, S. Fornarini, D. Scuderi, J.-Y. Salpin, Undervalued N3 Coordination Revealed in the Cisplatin Complex with 2′-Deoxyadenosine-5′-monophosphate by a Combined IRMPD and Theoretical Study, Inorg. Chem. 56 (2017) 8793–8801. doi:10.1021/acs.inorgchem.7b00570.

[44] D. Corinti, C. Coletti, N. Re, B. Chiavarino, M.E. Crestoni, S. Fornarini, Cisplatin Binding to Biological Ligands Revealed at the Encounter Complex Level by IR Action Spectroscopy, Chem. - A Eur. J. 22 (2016) 3794–3803. doi:10.1002/chem.201504521.

[45] D. Corinti, C. Coletti, N. Re, R. Paciotti, P. Maître, B. Chiavarino, M.E. Crestoni, S. Fornarini, Short-lived intermediates (encounter complexes) in cisplatin ligand exchange elucidated by infrared ion spectroscopy, Int. J. Mass Spectrom. 435 (2019) 7–17. doi:10.1016/j.ijms.2018.10.012.

[46] C.C. He, L.A. Hamlow, B. Kimutai, H.A. Roy, Z.J. Devereaux, N.A. Cunningham, J. Martens, G. Berden, J. Oomens, C.S. Chow, M.T. Rodgers, Structural determination of arginine-linked cisplatin complexes via IRMPD action spectroscopy: arginine binds to platinum via NO − binding mode, Phys. Chem. Chem. Phys. 23 (2021) 21959–21971. doi:10.1039/D1CP03407C.

[47] B. Kimutai, C.C. He, A. Roberts, M.L. Jones, X. Bao, J. Jiang, Z. Yang, M.T. Rodgers, C.S. Chow, Amino acid-linked platinum(II) compounds: non-canonical nucleoside preferences and influence on glycosidic bond stabilities, JBIC J. Biol. Inorg. Chem. 24 (2019) 985–997. doi:10.1007/s00775-019-01693-y.

[48] C.C. He, B. Kimutai, X. Bao, L. Hamlow, Y. Zhu, S.F. Strobehn, J. Gao, G. Berden, J. Oomens, C.S. Chow, M.T. Rodgers, Evaluation of Hybrid Theoretical Approaches for Structural Determination of a Glycine-Linked Cisplatin Derivative via

Infrared Multiple Photon Dissociation (IRMPD) Action Spectroscopy, J. Phys. Chem. A. 119 (2015) 10980–10987. doi:10.1021/acs.jpca.5b08181.

[49] Stewart, D. E., Sarkar, A. & Wampler, J. E. (1990).Occurrence and role of cis peptide bonds in protein structures. J. Mol. Biol. 214, 253-260. doi: 10.1016/0022-2836(90)90159-J.

[50] Weiss, M., Jabs, A. & Hilgenfeld, R. Peptide bonds revisited. Nat Struct Mol Biol 5, 676 (1998). https://doi.org/10.1038/1368

[51] S. Osburn, G. Berden, J. Oomens, R.A.J. O'Hair, V. Ryzhov, S-to-AC radical migration in the radical cations of gly-cys and cys-gly, J. Am. Soc. Mass Spectrom. 23 (2012) 1019–1023. doi:10.1007/s13361-012-0356-4.

[52] S. Osburn, G. Berden, J. Oomens, K. Gulyuz, N.C. Polfer, R.A.J. O'Hair, V. Ryzhov, Structure and reactivity of the glutathione radical cation: Radical rearrangement from the cysteine sulfur to the glutamic acid α-carbon atom, Chempluschem. 78 (2013) 970–978. doi:10.1002/cplu.201300057.

[53] B. Gregori, L. Guidoni, B. Chiavarino, D. Scuderi, E. Nicol, G. Frison, S. Fornarini, M.E. Crestoni, Vibrational signatures of S-nitrosoglutathione as gaseous, protonated species, J. Phys. Chem. B. 118 (2014) 12371–12382. doi:10.1021/jp5072742.

[54] N. Nieuwjaer, A. Beydoun, F. Lecomte, B. Manil, D. Scuderi, C. Desfrançois, Ligand-protected gold nanoclusters probed by IRMPD spectroscopy and quantum chemistry calculations, J. Mol. Spectrosc. 383 (2022) 111562. doi:10.1016/j.jms.2021.111562.

[55] J.M. Bakker, T. Besson, J. Lemaire, D. Scuderi, P. Maître, Gas-Phase Structure of a π-Allyl−Palladium Complex: Efficient Infrared Spectroscopy in a 7 T Fourier

Transform Mass Spectrometer, J. Phys. Chem. A. 111 (2007) 13415–13424. doi:10.1021/jp074935e.

[56] J.S. Prell, J.T. O'Brien, E.R. Williams, IRPD spectroscopy and ensemble measurements: Effects of different data acquisition and analysis methods, J. Am. Soc. Mass Spectrom. 21 (2010) 800–809. doi:10.1016/j.jasms.2010.01.010.

[57] P. Pracht, F. Bohle, S. Grimme, Automated exploration of the low-energy chemical space with fast quantum chemical methods, Phys. Chem. Chem. Phys. 22 (2020) 7169–7192, https://doi.org/10.1039/C9CP06869D

[58] M.J. Frisch, G.W. Trucks, H.B. Schlegel, G.E. Scuseria, M.A. Robb, J.R. Cheeseman, G. Scalmani, V. Barone, B. Mennucci, G.A. Petersson Gaussian 09, Revision D.01; Gaussian Inc.: Wallingford, CT, USA, 2009.

[59] Fedorov DG, Kitaura K (2007) Extending the power of quantum chemistry to large systems with the fragment molecular orbital method. J Phys Chem A 111:6904–6914. https://doi.org/10.1021/jp0716740

[60] Fedorov DG, Kitaura K (2006) The three-body fragment molecular orbital method for accurate calculations of large systems. Chem Phys Lett 433:182–187. https://doi.org/10.1016/j.cplett.2006.10.052

[61] Ishikawa T, Kuwata K (2009) Fragment molecular orbital calculation using the RI-MP2 method. Chem Phys Lett 474:195–198. https://doi.org/10.1016/j.cplett.2009.04.045

[62] Pham BQ, Gordon MS (2020) Development of the FMO/RI-MP2 fully analytic gradient using a hybrid-distributed/shared memory programming model. J Chem Theory Comput 16:1039–1054. https://doi.org/10.1021/acs.jctc.9b01082

[63] Mori H, Ueno-Noto K, Osanai Y, Noro T, Fujiwara T, Klobukowski M, Miyoshi E (2009) Revised model core potentials for third-row transition–metal atoms from Lu to Hg. Chem. Phys. Lett. 476:317–322. https://doi.org/10.1016/j.cplett.2009.06.019

[64] D. G. Fedorov, L. V. Slipchenko, K. Kitaura, Systematic Study of the Embedding Potential Description in the Fragment Molecular Orbital Method, J. Phys. Chem. A 114 (2010) 8742–8753. https://doi.org/10.1021/jp101724p

[65] D. G. Fedorov, K. Kitaura, Pair interaction energy decomposition analysis. J Comput Chem 28 (2007) 222–237. https://doi.org/101002/jcc.20496

[66] R. Paciotti, L. Storchi, A. Marrone, Homodimeric complexes of the 90–231 human prion: a multilayered computational study based on FMO/GRID-DRY approach, J. Mol. Model 28 (2022) 241. https://doi.org/10.1007/s00894-022-05244-2

[67] R. Paciotti, L. Storchi, A. Marrone, An insight of early PrP-E200K aggregation by combined molecular dynamics/fragment molecular orbital approaches, Proteins. 87 (2019) 51–61. https://doi.org/10.1002/prot.25621

[68] L. Storchi, R. Paciotti, N. Re, A. Marrone, Investigation of the molecular similarity in closely related protein systems: The PrP case study, Proteins. 83 (2015) 1751–1765. https://doi.org/10.1002/prot.24836

[69] R. Paciotti, M. Agamennone, C. Coletti, L. Storchi, Characterization of PD-L1 binding sites by a combined FMO/GRID-DRY approach, J. Comput. Aided. Mol. Des. 34 (2020) 897–914. doi:10.1007/s10822-020-00306-0.

[70] R. Paciotti, C. Coletti, A. Marrone, N. Re, The FMO2 analysis of the ligand-receptor binding energy: the Biscarbene-Gold(I)/DNA G-Quadruplex case study, J. Comput. Aided. Mol. Des. 36 (2022) 851–866. doi:10.1007/s10822-022-00484-z.

[71] D.G. Fedorov, Three-Body Energy Decomposition Analysis Based on the Fragment Molecular Orbital Method, J. Phys. Chem. A. 124 (2020) 4956–4971. doi:10.1021/acs.jpca.0c03085.

[72] G.M.J. Barca, C. Bertoni, L. Carrington, D. Datta, N. De Silva, J.E. Deustua, D.G. Fedorov, J.R. Gour, A.O. Gunina, E. Guidez, T. Harville, S. Irle, J. Ivanic, K. Kowalski, S.S. Leang, H. Li, W. Li, J.J. Lutz, I. Magoulas, J. Mato, V. Mironov, H. Nakata, B.Q. Pham, P. Piecuch, D. Poole, S.R. Pruitt, A.P. Rendell, L.B. Roskop, K. Ruedenberg, T. Sattasathuchana, M.W. Schmidt, J. Shen, L. Slipchenko, M. Sosonkina, V. Sundriyal, A. Tiwari, J.L. Galvez Vallejo, B. Westheimer, M. Włoch, P. Xu, F. Zahariev, M.S. Gordon, Recent developments in the general atomic and molecular electronic structure system, J. Chem. Phys. 152 (2020) 154102. doi:10.1063/5.0005188.

[73] A. De Petris, A. Ciavardini, C. Coletti, N. Re, B. Chiavarino, M.E. Crestoni, S. Fornarini, Vibrational signatures of the naked aqua complexes from platinum(II) anticancer drugs, J. Phys. Chem. Lett. 4 (2013) 3631–3635. doi:10.1021/jz401959s.

[74] R. Wu, T.B. McMahon, Infrared multiple photon dissociation spectroscopy as structural confirmation for GlyGlyGlyH+ and AlaAlaAlaH+ in the gas phase. Evidence for amide oxygen as the protonation site, J. Am. Chem. Soc. 129 (2007) 11312–11313. doi:10.1021/ja0734492.

[75] R. Wu, T.B. McMahon, Protonation sites and conformations of peptides of glycine (Gly 1-5H+) by IRMPD spectroscopy, J. Phys. Chem. B. 113 (2009) 8767–8775. doi:10.1021/jp811468q.

[76] J. K. Martens, J. Grzetic, G. Berden, J. Oomens Gas-phase conformations of small polyprolines and their fragment ions by IRMPD spectroscopy International Journal of Mass Spectrometry 377 (2015) 179–187

[77] H. Li, J. Jiang, Y. Luo Identification of the protonation site of gaseous triglycine: the cis-peptide bond conformation as the global minimum Phys. Chem. Chem. Phys., 2017, 19, 15030 doi:10.1039/C7CP01997A

[78] Z. Chval, M. Sip, J. V. Burda The Trans Effect in Square-Planar Platinum(II) Complexes—A Density Functional Study J Comput Chem 29: 2370–2381, 2008 https://doi.org/10.1002/jcc.20980